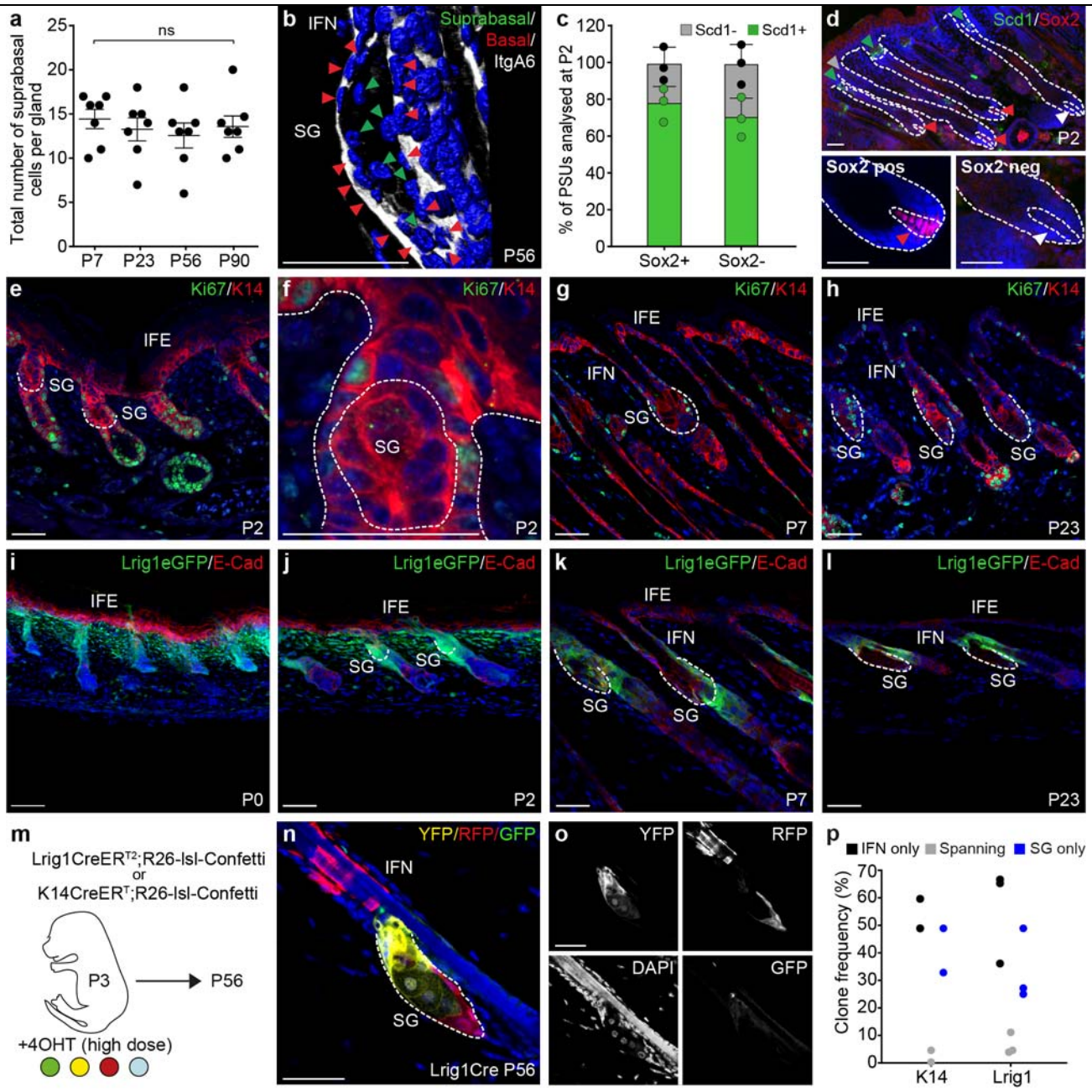

Supplementary Figure 1

Patterning of the upper pilosebaceous unit

(**a**) Number of suprabasal (ItgA6 negative) cells in the SG at indicated time points. Lines represent mean±S.E.M. Mann Whitney two tailed statistical test used. n=7 glands for all time points. (**b**) Representative image for the quantification in (**a**). SG and IFN demarcated, ItgA6 positive SG basal

cells (red arrows) and ItgA6 negative suprabasal cells (green arrows) respectively. Image representative of 7 glands. (**c**) Percentage at P2 of awl/auchene hair follicles (distinguished by presence of Sox2+ cells in the dermal papillae) and zig zag hair follicles (Sox2- dermal papillae) that have SCD1 positive cells in the site demarcating the prospective sebaceous gland bud, data displayed as mean±S.D. Number of follicles counted Sox2-=41, Sox2+=39 in n=3 animals for each group. (**d** Top panel) Representative images of the quantification in (**c**) individual hair follicles are outlined with dotted lines, as well as the dermal papillae and the prospective site of SG morphogenesis. Red arrows indicate awl/auchene hair follicles, while the white arrow indicate a zig zag hair follicle. Green arrows indicate follicles positive for SCD1 cells (green arrows) or SCD1 negative cells (grey arrows). (**d** Bottom panel) Close up images of Sox2+ and Sox2- dermal papilla of awl/auchene and zig zag hairs. Images representative of 3 mice. (**e-h**) Representative images of Ki67 (green) and K14 (red) during gland formation P2 (e,f), end of morphogenesis P7 and homeostasis P23, n=3 animals per time point. (**i-l**) Detection of Lrig1eGFP (green) and E-Cadherin (E-cad, red) at P2, P7 and P23, n=3 animals per time point. (**m**) Strategy for pulse-chase clonal labelling experiments with high dose of 4OHT. (**n**) Detection of GFP (green), YFP (yellow) and RFP (red) patches of labelled cells in rendered confocal z-stacks of back skin from the Lrig1CreER^{T2}-based mouse model experiment outlined in (**m**). (**o**) Same as (**n**) but each channel in grey scale, 3 animals per time point. (**p**) Patch frequency in individual animals according to patch-location within the SG, IFN or both (spanning) following labelling of either K14 or Lrig1 expressing cells. Each dot represents an independent animal. Nuclei are counterstained with DAPI (blue). Scale bars, 50μm.

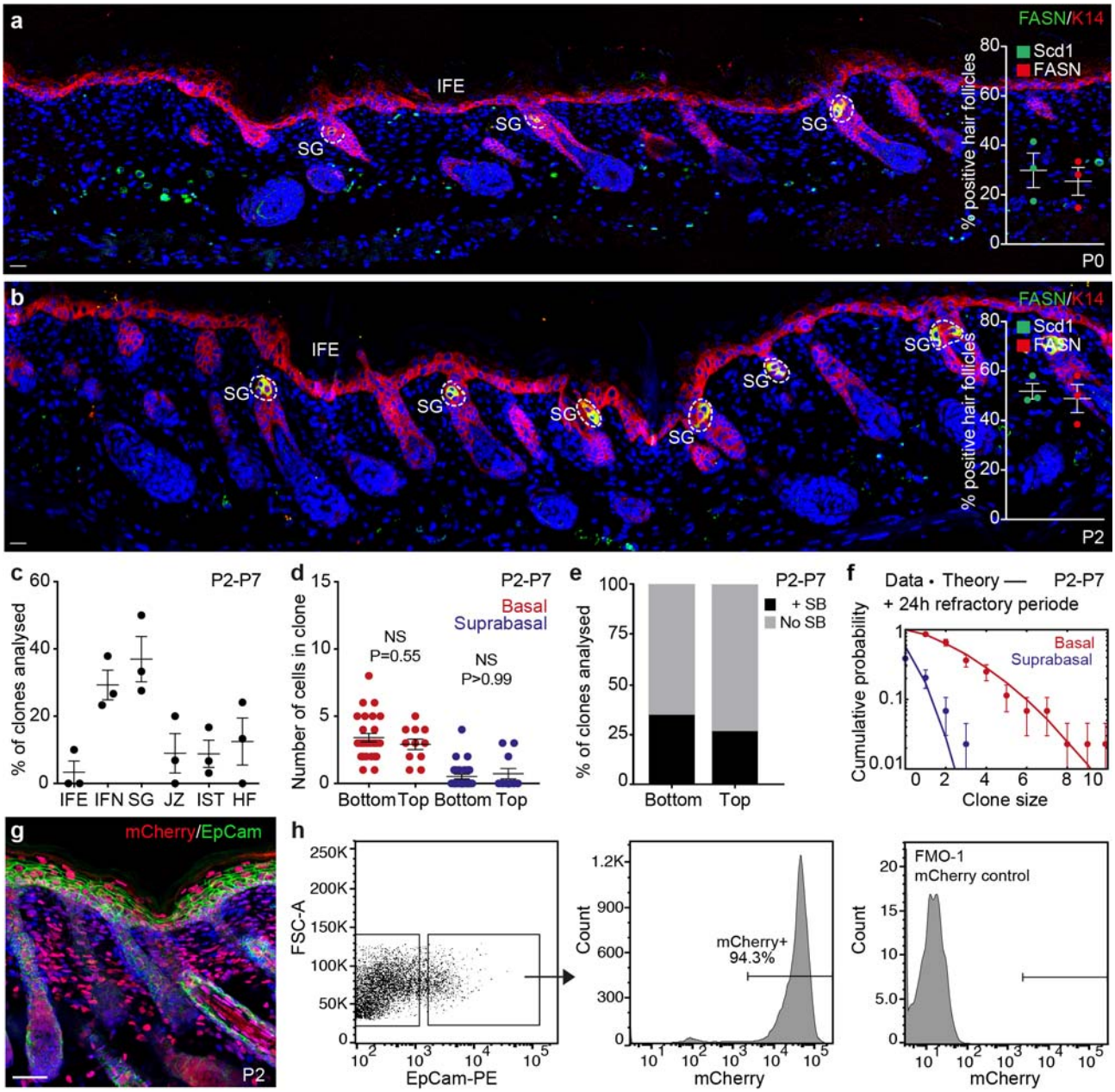

Supplementary Figure 2

Characterisation of sebaceous gland formation

(**a, b**) Detection of K14 (red) and FASN (green) in P0 and P2 mouse epidermis and frequency of hair follicles with cells positive for FASN and Scd1. Lines represent mean±S.E.M. from n= 3 animals (Number of hair follicles analysed: P0: 35, 80 and 32; P2: 39, 46 and 29). (**c**) Localisation of clones at

P7 following induction at P2. Lines represent mean±S.E.M. for n=3 animals and 30 clones counted per animal. (**d**) SG clone size at P7 divided into their respective location; top or bottom part of the gland. Lines represent mean±S.E.M. (Top: n=11 clones and Bottom: n=27 clones from 5 mice, basal and suprabasal cells). Mann Whitney two tailed statistical test used (**e**) Relative frequency of clones in the upper and the lower sebaceous gland at P7 that either contain suprabasal (+SB) or lack suprabasal (No SB) cells. (Top: n=11 clones and Bottom: n=27 clones from 5 mice). (**f**) Biophysical modelling based on a single equipotent progenitor model, using data from Figure 2d but introducing a 24h refractory period between individual cell cycles, an improved fit to the clonal fate data for both basal (red) and suprabasal (blue) clone size distribution at P7, by explaining the slight deviation from exponential behaviour at small clone sizes. Error bars are mean±S.E.M. (**g**) Detection of EpCam (green) and H2BmCherry (red) in back skin from the Col1a1-tetO-H2BmCherry mouse model at P2 following a 2-week doxycycline (dox) pulse. Image representative of 3 animals. (**h**) Flow cytometric analysis of cells isolated from dox pulse back skin samples from P2. Epithelial cells were analysed for mCherry expression in the $CD31^{neg}/CD45^{neg}/EpCam^{pos}$ cell fraction. $CD31^{neg}/CD45^{neg}/EpCam^{pos}$ cells from wild type littermates where used for Fluorescence Minus One (FMO-1) control to indicate mCherry negative cut off levels. Images representative of 3 animals. Nuclei are counterstained with DAPI (blue). Scale bars, 50μm.

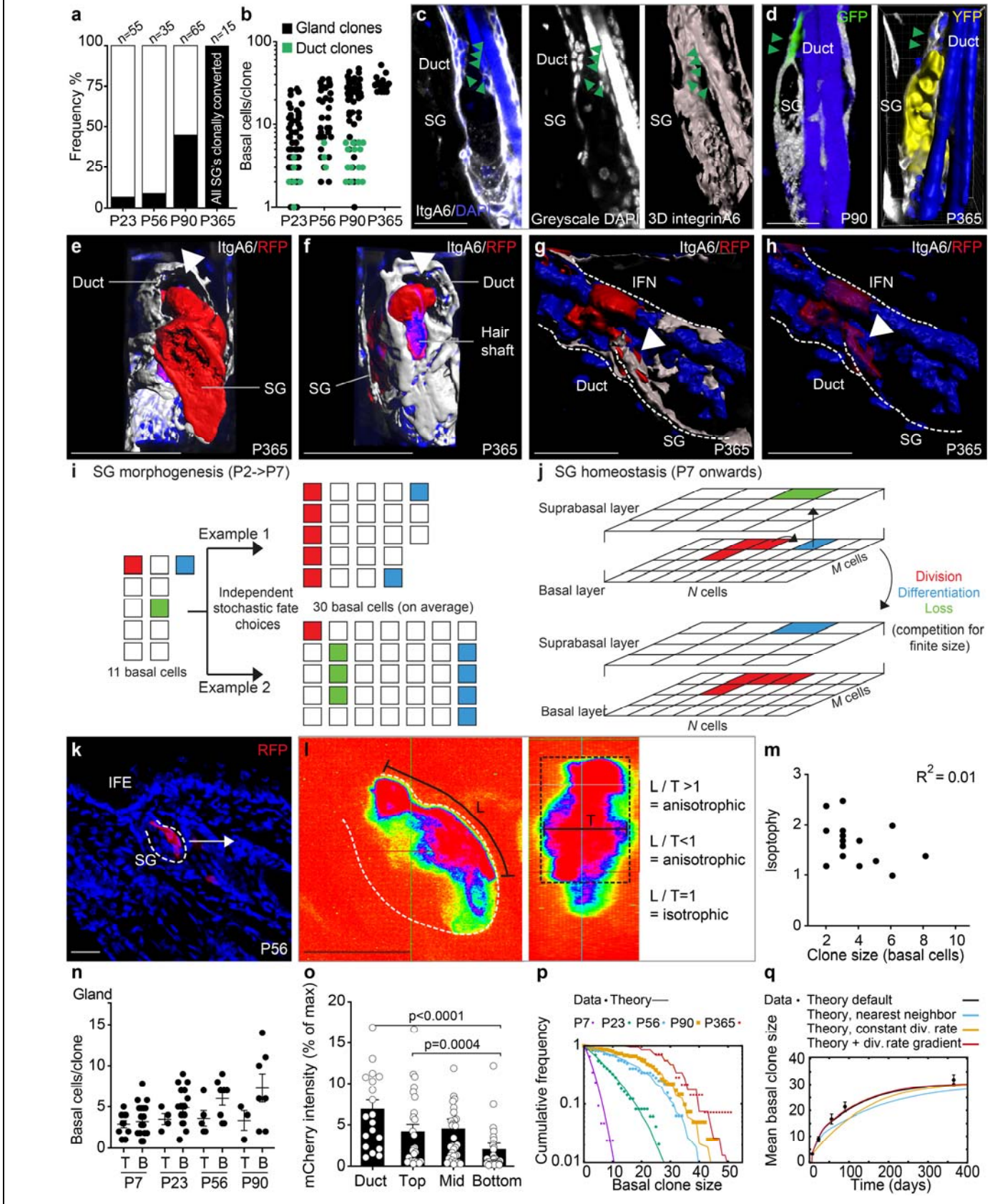
a
b
c
d
e
f
g
h
i SG morphogenesis (P2->P7)
j SG homeostasis (P7 onwards)
k
l
m
n
o
p
q
Frequency %
All SGs clonally converted
Gland clones
Duct clones
Basal cells/clone
P23 P56 P90 P365
Duct
SG
ItgA6/DAPI
Greyscale DAPI
3D integrinA6
GFP
YFP
P90
P365
ItgA6/RFP
Hair shaft
IFN
Example 1
Example 2
Independent stochastic fate choices
11 basal cells
30 basal cells (on average)
Suprabasal layer
Basal layer
M cells
N cells
Division
Differentiation
Loss
(competition for finite size)
RFP
IFE
L / T >1 = anisotrophic
L / T<1 = anisotrophic
L / T=1 = isotrophic
R2 = 0.01
Isoptophy
Clone size (basal cells)
Gland
T B
P7 P23 P56 P90
mCherry intensity (% of max)
p<0.0001
p=0.0004
Duct Top Mid Bottom
Data • Theory
Cumulative frequency
Basal clone size
Theory default
Theory, nearest neighbor
Theory, constant div. rate
Theory + div. rate gradient
Mean basal clone size
Time (days)

Supplementary Figure 3

Maintenance of the adult sebaceous gland

(a) Clonally converted SGs at the indicated time points. Total number of clones (n) analysed are indicated as 100% bars with actual numbers on top (**b**) Size of clones located in the duct (green arrows). P23; n=6 duct clones out of 49 in total, P56; n=3 duct clones out of 32, P90; n=15 duct clones out of 68, P365; n=0 duct clones out of 15. (**c**) Detection of ItgA6 (white) in adult P56 SGs. Arrowheads indicate duct cells. (**d**) Representative clones of the duct (GFP) or gland (YFP) with the duct demarcated (arrowheads). (**e, f**) Diagonal 3D reconstituted views of a SG clone (RFP) with negative duct (arrowhead). (**g, h**) infundibulum clone with duct contribution (arrowhead). (e-g) Counterstained with ItgA6 (white). (**i, j**) Biophysical modelling principles for SG homeostasis, starting from morphogenesis with niche size being fixed from P7 (see Supplementary Note). (**k-l**) Example of isotropy analysis of SG clones projected according to colour intensity. L=longitudinal and T=transverse clone axis. (**m**) Isotropy measurements for SG-clones at P56 and respective R square value following linear regression analysis. n=16 clones measured (**n**) Number of basal cells lining the longitudinal axis exclusively in the SG top 1/3 (T) or bottom 1/3 (B), (P7; top-n=11, bottom-n=27 out of 44 clones measured, P23; top-n=4, bottom-n=18 out of 49, P56; top-n=5, bottom-n=8 out of 32; P90; top-n=3, bottom-n=7 out of 68 (**o**) Quantification of H2BmCherry fluorescence intensity of basal cell nuclei following a 9-day chase relative to the median fluorescence intensity of non-chased (max) animals (Duct-n=40 nuclei; Top-n=59; Mid-n=58; Bottom-n=53); 9-day chase: Duct-n=45; Top-n=59; Mid-n=80; Bottom-n=80. Data pooled from 3 animals for each group. Mann Whitney two tailed statistical test used (**p**) Model prediction using parameters extracted in (3l). Curves individually fitted to the simulated time point with corresponding average. Line represents the model prediction and basal clone size distribution, points represent clones analysed at indicated time points. (**q**) Model predictions for basal clone size distribution (data from figure 3l (black line)). Testing underlying dynamics hypothesises: loss-replacement of nearest neighbours only (blue), an instantaneous decrease in division time from 1.7 days before P7 to 3.5 days after P7 (orange) and a 25% gradient of division rates along the bottom-up SG axis (red). Data displayed are mean±S.E.M. Statistical significance tested using non-paired Mann-Whitney test. Nuclei stained with DAPI (blue). Scale bars, 50μm.

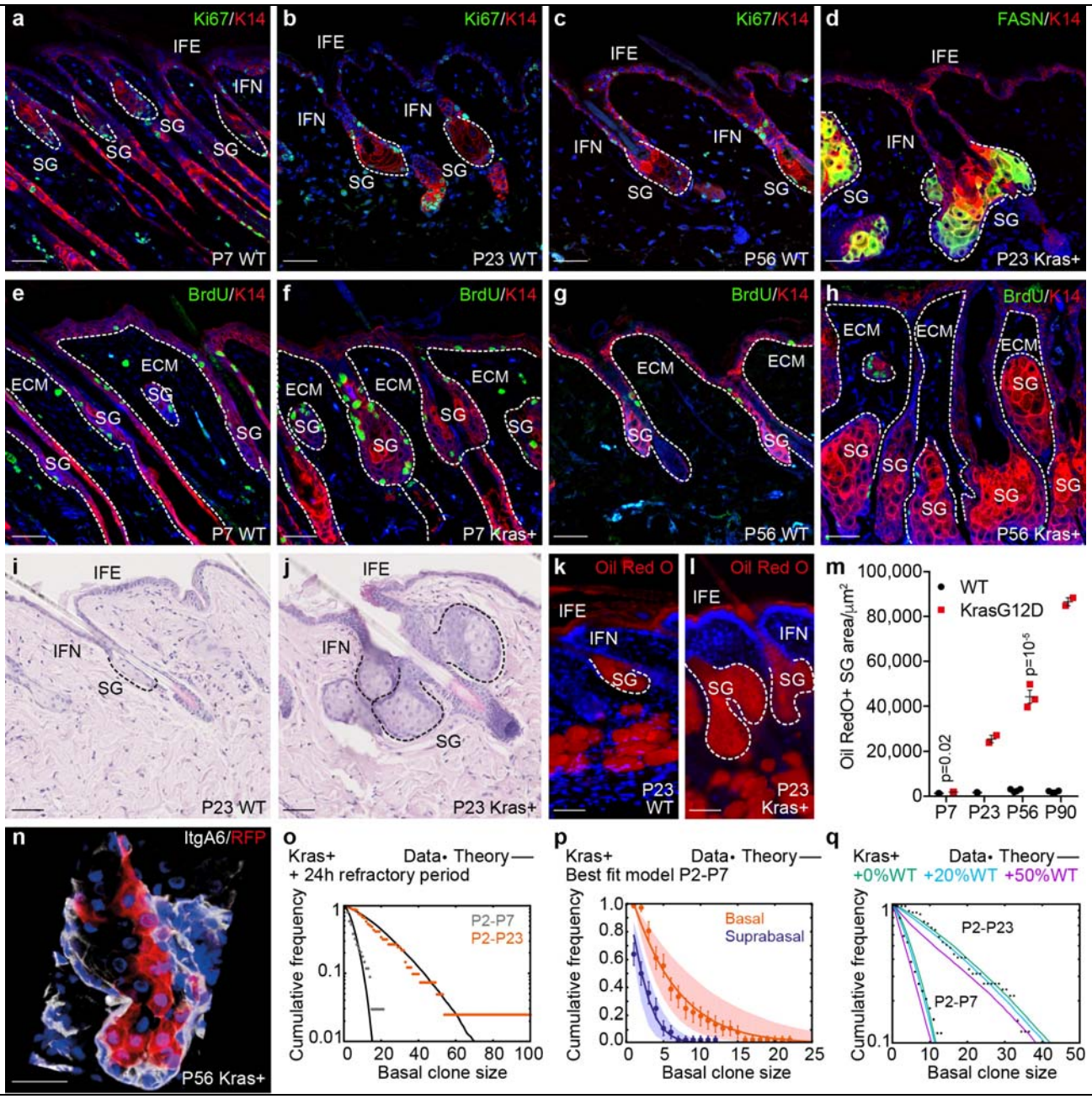

Supplementary Figure 4

Sebaceous gland function is maintained upon KrasG12D activation

(**a-c**) Detection of Ki67 (green) and K14 (red) in WT tissue at indicated time-points. 3 animals per group. (**d**) Detection of FASN (green) and K14 (red) in KrasG12D expressing SG. 3 animals per group (**e-h**) Detection of BrdU (green) and K14(red) after a single pulse in WT and KrasG12D mutant mice at P7 and P56 n=3 animals per group. (**i, j**) Back skin tissue section from P23 stained with hematoxylin and Eosin from either WT or KrasG12D expressing mouse back skin at P23. Images representative of 3 animals per group. (**k, l**) Detection of lipids by Oil Red O (red) in back skin of WT and KrasG12D mutant mice at P23. Images representative of 3 animals per group. (**m**) SG size

measurements according to Oil Red O surface area (μm^2). Dots represent average measurements from independent animals (WT P7 n=3; P23 n=3; P56 n=4; P90 n=4; KrasG12D P7 n=3; P23 n=2; P56 n=3; P90 n=2). Data displayed are mean±S.E.M and statistical significance tested unpaired two-way students t-test. (**n**) Detection of clone (red) in a rendered confocal z-stack from KrasG12D tissue counterstained for IntegrinA6 (ItgA6, white). Image representative of 3 animals. (**o**) Fit of the basal clone size distributions with the same parameters as Figure 5m, but incorporating a small refractory period until the next division, providing a slightly improved fit (solid lines). Basal clone size distribution of cohorts analysed at P7 (grey) and P23 (orange) are indicated (measurement are from Figure 5i,j). (**p**) Basal (red) and suprabasal (blue) clone size distribution at P7 after a P2 induction, together with the corresponding best-fit predictions from a stochastic model of an equipotent imbalance progenitor population (used to extract the P2-P7 parameters of Figure 5k). Lines and shaded areas represent best-fit predictions and 95% confidence interval respectively. (o,p) KrasG12D: P7-n=34 clones from 3 animals; P23-n=41 clones from 4 animals. (**q**) Numerical simulation of clone size distributions at P7 and P23 for a P2 induction based on a model of mixed KrasG12D and WT cells. Data is shown as dots (black: P7, red: P23) and models with different fractions f as lines (f=0% in green, f=20% in cyan, f=50% in purple). The model diverges from the data (in particular at P23) as f increases. Scale bars, 50μm.

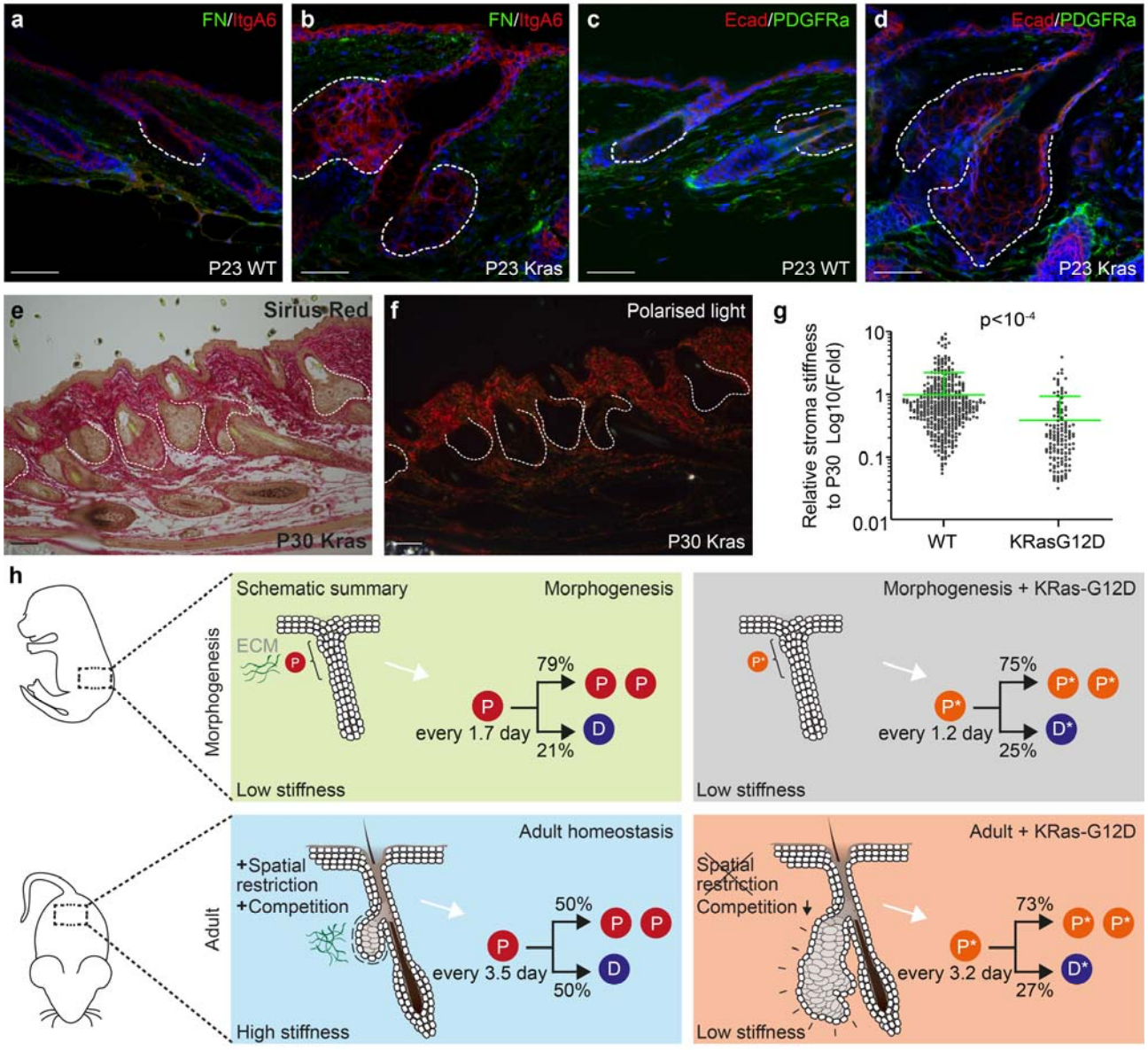

Supplementary Figure 5

Effect of KrasG12D mutation on matrix surrounding the sebaceous gland

(**a,b**) Fibronectin and (**c,d**) PDGFRa staining in WT and KrasG12D mutant animals at P23 (a-d). Images representative of 3 animals. (**e**) Sirius red staining of back skin sections for collagen deposition in brightfield and **(f)** fibrillisation visualized using polarized light microscopy in samples from mice with KrasG12D mutation. Images representative of 2 animals. Sebaceous glands outlined with dotted line. (**g**) Atomic force microscopy measurement of elastic modulus in the stroma surrounding the SG using a spherical probe in WT and KrasG12D mice at P30. Data displayed as a scattered dot plot with line indicating mean and error bar representing S.D. WT: n=395 individual measurements pooled from 3 animals, KrasG12D: n=137 individual measurements, pooled from 2 animals. Significance was estimated based on a Kruskal-Wallis test. (**h)** Schematic summary. Nuclei are counterstained with DAPI (blue). Scale bars, 50μm.
Supplementary Table 1
Differentially expressed genes between morphogenesis and homeostatic states.
List of differentially expressed genes (Log2fold change > 0.5; FDR < 0.05 based on Benjamini-Hochberg multiple correction method following a Wald test for statistical significance) between P4 – P10, and P4 – P30 time points. n=3 animals per group.
Supplementary Table 2
Antibodies used for immunofluorescence and immunohistochemistry.
Supplementary Table 3
Source data for all figures.
Supplementary Note
Detailed description of the biophysical modelling of the quantitative fate mapping data.